Disulfide Bond-Dependent Mechanism of Protection against Oxidative Stress in Pyruvate-Ferredoxin Oxidoreductase of Anaerobic *Desulfovibrio* Bacteria

Nicolas Vita, E. Claude Hatchikian, Matthieu Nouailler,‡ Alain Dolla, and Laetitia Pieulle*

Laboratoire de Bioénergétique et Ingénierie des Protéines, Unité Propre de Recherche (UPR) 9036, Centre National de la Recherche Scientifique (CNRS) 31, Chemin Joseph Aiguier, 13402 Marseille, cedex 20, France

Received July 25, 2007; Revised Manuscript Received October 16, 2007

ABSTRACT: Oxidative decarboxylation of pyruvate forming acetyl-coenzyme A is a crucial step in many metabolic pathways. In most anaerobes, this reaction is carried out by pyruvate-ferredoxin oxidoreductase (PFOR), an enzyme normally oxygen sensitive except in *Desulfovibrio africanus* (*Da*), where it shows an abnormally high oxygen stability. Using site-directed mutagenesis, we have specified a disulfide bond-dependent protective mechanism against oxidative conditions in *Da* PFOR. Our data demonstrated that the two cysteine residues forming the only disulfide bond in the as-isolated PFOR are crucial for the stability of the enzyme in oxidative conditions. A methionine residue located in the environment of the proximal [4Fe-4S] cluster was also found to be essential for this protective mechanism. In vivo analysis demonstrated unambiguously that PFOR in *Da* cells as well as two other *Desulfovibrio* species was efficiently protected against oxidative stress. Importantly, a less active but stable *Da* PFOR in oxidized cells rapidly reactivated when returned to anaerobic medium. Our work demonstrates the existence of an elegant disulfide bond-dependent reversible mechanism, found in the *Desulfovibrio* species to protect one of the key enzymes implicated in the central metabolism of these strict anaerobes. This new mechanism could be considered as an adaptation strategy used by sulfate-reducing bacteria to cope with temporary oxidative conditions and to maintain an active dormancy.

The oxidative decarboxylation of pyruvate is a fundamental part of metabolic pathways in living organisms in general. Two types of thiamine pyrophosphate (TPP)[1]-dependent enzymatic systems catalyze this reaction: (i) the pyruvate dehydrogenase multienzyme complex in mitochondria and most aerobic bacteria using NAD^+ as the electron acceptor and (ii) the single enzyme pyruvate-ferredoxin oxidoreductase (PFOR) found in most anaerobes using acceptors with more negative potentials, such as ferredoxins (Fd), to transfer electrons. In the latter case, the corresponding reaction is $CH_3\text{-}CO\text{-}COO^- + 2Fd_{ox} + CoA \leftrightarrows CH_3\text{-}CO\text{-}CoA + 2Fd_{red} + CO_2$. In strictly anaerobic organisms and anaerobic protozoa, PFOR is involved in a phosphoroclastic reaction allowing energy conservation by substrate-level phosphorylation. Furthermore, the enzyme can carry out the reverse reaction to yield pyruvate, constituting the basis for CO_2 fixation in various microorganisms (*1*−*5*). Although PFORs have different oligomeric structures, they are all phylogenetically closely related (*6*, *7*). In addition to the site of pyruvate decarboxylation, TPP, all PFOR enzymes contain up to three iron-sulfur clusters, providing a potential electron-transfer pathway.

PFORs from most anaerobes are typically unstable in vitro toward oxygen, although this is not universally true. The PFOR found in *Desulfovibrio africanus* (*Da*) provides an intriguing exception to this rule (*8*). Bacteria of the genus *Desulfovibrio* exhibit a unique strictly anaerobic mode of growth based on the reduction of sulfate as the terminal electron acceptor. In the presence of sulfate, pyruvate is a key intermediate during oxidation of organic substrates such as lactate or fumarate into acetate (*9*). In addition, pyruvate is a well-known fermentative substrate for sulfate reducers. The energy metabolism of *Desulfovibrio* highlights PFOR as a crucial enzyme for these organisms. In *Da*, PFOR is a homodimeric protein with a molecular mass of 266 kDa and shows an unusual stability for several days (*8*) when isolated under aerobic conditions, thus enabling extensive studies (*8*, *10*−*13*). As determined by X-ray crystallography (*12*), its structure contains one TPP molecule per subunit buried in the protein and three $[4Fe\text{-}4S]^{2+/1+}$ clusters with midpoint potentials ranging from −540 to −390 mV (*8*, *12*). The reaction mechanism of the PFOR in *Da* involves the formation of a stable free radical reaction intermediate (*8*, *14*). The activity of the pure enzyme increases approximately 5-fold in the presence of sulfhydryl agents such as dithioerythritol (DTE), although the enzyme becomes air-sensitive and is irreversibly inactivated in air (*8*). This loss of activity is accompanied by a bleaching of the protein solution consistent with cluster disintegration. The sensitivity to aeration is thought to be due to solvent exposure of at least one cluster, triggered by the reduction of a putative disulfide bridge in the C-terminal region. Drastic effects on oxygen

* Corresponding author. Phone: 33-4-91-16-44-94; fax: 33-4-91-16-45-78; e-mail: pieulle@ibsm.cnrs-mrs.fr.

‡ Present address: Architecture et Fonction des Macromolécules Biologiques, Unité Mixte de Recherches (UMR) 6098, CNRS, Case 932, 163 Avenue de Luminy, 13288 Marseille cedex 9, France.

[1] Abbreviations: PFOR, pyruvate-ferredoxin oxidoreductase; TPP, thiamine pyrophosphate; *Da*, *Desulfovibrio africanus*; DTE, dithioerythritol; *Dv*H, *Desulfovibrio vulgaris* Hildenboroug; *Dd* G20, *Desulfovibrio desulfuricans* G20; *Ca*, *Clostridium acetobutylicum*; MV, methyl viologen.

10.1021/bi7014713 CCC: $40.75
Published on Web 12/28/2007

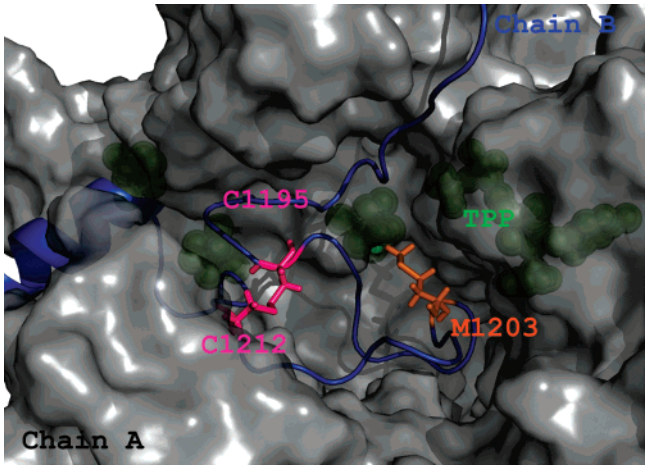

FIGURE 1: Ribbon representation of the C-terminal domain of the *Da* PFOR (chain B, in blue), located in the groove at the surface of the other subunit represented in the van der Waals surface (chain A, in gray). The three clusters [4Fe-4S] and the thiamine-pyrophosphate (TPP) cofactor of chain A are green. In chain B, the side chain of the two Cys (C1195 and C1212) residues involved in the disulfide bond and that of Met 1203 are pink and orange, respectively. The figure was drawn with Pymol 0.95 (*42*).

stability caused by truncations of the C-terminal part of PFOR from *Da* support this idea (*10*). The crystal structure of the *Da* PFOR isolated under aerobic conditions confirmed the existence of this disulfide bridge and also showed that the C-terminal end of one subunit occluded the proximal cluster of the other through the involvement of a methionine residue (Figure 1, ref *12*). This unique conformation allowing exclusion of the solvent from the vicinity of the proximal cluster could be responsible for the stability of PFOR to oxygen, thus protecting it from oxidative damage.

For the present study, we used site-directed mutagenesis on PFOR from *Da* to specify at the molecular level this disulfide bond-dependent protective mechanism. Moreover, we report that in vivo, this mechanism efficiently provides a reversible disulfide bond controlled switch from a protected and partially active form of the enzyme to a fully active form, depending on the oxidation state of the environment.

EXPERIMENTAL PROCEDURES

Bacterial Strains and Growth Conditions. The *Da* strain Benghazi (NCIB 8401) was grown anaerobically at 37 °C in a basic lactate-sulfate medium as previously described (*15*) containing 36 mM sulfate and 80 mM lactate. *Desulfovibrio vulgaris* Hildenborough (*Dv*H, ref 16) and *Desulfovibrio desulfuricans* G20 (*Dd*G20, ref 17) were cultured at 32 °C in medium C (*16*). *Clostridium acetobutylicum* ATCC 824 (*Ca*) was grown at 37 °C in 2YT medium containing 5 g of glucose per liter in anaerobic conditions. *Escherichia coli* DH5α was used for plasmid propagation and *E. coli* TG1 for heterologous expression of the *Da por* gene (*10*). Growth medium was supplemented with ampicillin (100 μg/mL) when appropriate.

Specific Amplification of the 3′ End por Genes from Desulfovibrio Species, Cloning, and Sequencing. A pair of degenerate oligonucleotides was designed from the C-terminal amino acid sequence of *Da* PFOR (d and drev, Table 1). PCR amplification was performed with the Expand PCR System (Roche) using chromosomal DNA from *Desulfovibrio gigas* (*Dg*) and *Desulfovibrio fructosovorans* (*Df*) prepared with a genomic DNA purification kit (Promega). The TA cloning kit (Invitrogen) was used for cloning PCR products. Addition of 5% DMSO was supplied in the PCR mixtures because *Desulfovibrio* DNA is G + C rich. Amplification of flanking sequences by inverse PCR was carried out as described previously (*18*). PCR was performed using two outward-facing oligonucleotides (InvG and InvGr or InvG2 and InvG2r for the 3′ end of the *Dg por* gene and InvF and InvFr for the 3′ end of the *Df por* gene, Table 1). The inverse PCR products were directly sequenced.

Table 1: Oligonucleotide Primer DNA Sequence Used for Specific Amplification of 3′ End *Desulfovibrio por* Genes

Name	sequence[a]
d[b]	TgYATHCARTgYAAYCARTg
drev[b]	gCCCANCCRTCNCCNCCRAA
InvGr	gggTgAgCAgCTTgACgTAggg
InvG	gCAAgCTCTgCCCCACCCTgC
InvG2	ggACTTCCTgggCggCgAATCC
InvG2r	gTCCggggCCTTggAATCCAgC
InvFr	TTTTCCCgACgCTgCTTgAgg
InvF	CCTgCTCgACAAAAACgACCCgg

[a] Oligonucleotides are written in the usual 5′−3′ direction. [b] Universal nomenclature used to defined d and drev degenerated oligonucleotides are the following: R for A or G; Y for C or T; H for A, C, or T; and N for A, G, C, or T.

Site-Directed Mutagenesis of Da PFOR. All mutations were localized in the 3′ end of the *por* coding sequence. To construct mutant plasmids and to avoid undesired mutations, the 0.45 kb *Sac*II-*BamH*I fragment from pLP1 (*10*) was replaced by the same *Sac*II-*BamH*I fragment harboring the desired mutations. Mutations were introduced into this fragment by an overlapping PCR procedure (*19*) (Table 2). Constructions were then verified by sequencing.

Production of Da Molecular Variants of PFOR in E. coli and Preparation of Soluble Extracts. Recombinant wild type and variant PFORs were produced in *E. coli* TG1. Cells were grown anaerobically at 37 °C in 600 mL of modified Terrific Broth medium (Difco) with 20 mM fumarate. Before inoculation, the medium was supplemented with 100 mg/L ferric ammonium citrate, 1 mM L-Cys (*20*), and 100 mg/L ampicillin. When the culture reached 0.7 A_{600} units, production of PFOR was induced for 3 h with 0.4 mM isopropyl-β-d-thiogalactopyranoside. Cells were then harvested by centrifugation, and the pellet was washed with 50 mM Tris-HCl buffer (pH 8.5). The pellet was then gently resuspended in 10 mL of the same buffer containing a cocktail of protease inhibitors (Complete, Roche). Finally, the cells were passed once through a French pressure cell at 100 MPa, and the cell debris was removed by centrifugation at 30 000*g* for 20 min at 4 °C. This crude extract was then centrifuged at 120 000*g* for 90 min at 4 °C to obtain the soluble protein extract. This procedure of preparation is referred to hereafter as the oxidative condition. For the preparation of soluble extracts in anaerobic conditions, buffers were bubbled with argon for 30 min prior to utilization, and samples were manipulated in an anaerobic chamber. For disruption, cells were transferred to a French pressure cell equilibrated in the anaerobic chamber, and the extract was collected through an airtight system connected to the French pressure cell. The extract was then centrifuged in a closed centrifuge tube. The

Table 2: Template and Oligonucleotide Primer DNA Sequence Used in the Site-Directed Mutagenesis of *Da* PFOR[a]

Mutant	Template[1]	Oligonucleotide[2]
C1195A	*Da* DNA	p11 + GGCGTATCGTCGCGCGTG**GC**GAACTCCGCACCTTCG
		+
	pLP1	180re + CGAAGGTGCGGAGTTC**GC**CACGCGCGACGATACGCC
C1212A	*Da* DNA	p11 + CGCGGTTCTGGTCG**GC**GGCCTCACCGGAATCAGG
		+
	pLP1	180re + CCTGATTCCGGTGAGGCC**GC**CGACCAGAACCGCG
M1203E	*Da* DNA	p11 + GGAATCAGGTCGGGC**CTC**CATGGGCGTATCGTCG
		+
	pLP1	180re + CGACGATACGCCCATG**GAG**GCCCGACCTGATTCC
M1203H	*Da* DNA	p11 + GGAATCAGGTCGGGC**GTG**CATGGGCGTATCGTCG
		+
	pLP1	180re + CGACGATACGCCCATG**CAC**GCCCGACCTGATTCCG
M1203A	*Da* DNA	p11 + GGAATCAGGTCGGGC**TGC**CATGGGCGTATCGTCG
		+
	pLP1	180re + CGACGATACGCCCATG**GCA**GCCCGACCTGATTCCG
M1203L	*Da* DNA	p11 + GGAATCAGGTCGGGC**CAG**CATGGGCGTATCGTCG
		+
	pLP1	180re + CGACGATACGCCCATG**CTG**GCCCGACCTGATTCCG
M1203Y	*Da* DNA	p11 + GGAATCAGGTCGGGC**ATA**CATGGGCGTATCGTCG
		+
	pLP1	180re + CGACGATACGCCCATG**TAT**GCCCGACCTGATTCCG
M1203F	*Da* DNA	p11 + GGAATCAGGTCGGGC**AAA**CATGGGCGTATCGTCG
		+
	pLP1	180re + CGACGATACGCCCATG**TTT**GCCCGACCTGATTCCG

[a] 1: *Da* DNA for *Desulfovibrio africanus* genomic DNA. 2: Change made to the native sequence at the position indicated in bold and underlined capital letters. The mutagenic oligonucleotides are written in the usual 5′−3′ direction. p11: 5′-AAGAAGGACCTGGCGCGCATG-3′ and 180re: 5′-CCACACTACCATCGGCGCTACGG-3′.

protein concentration of the *E. coli* soluble extracts was between 15 and 20 mg/mL.

Exposure of Bacterial Cells to Air or H_2O_2. Cultures (80 mL) of *Da* cells were grown anaerobically in lactate-sulfate medium until the middle of the exponential growth phase. At that moment, the initial PFOR catalytic activity of the whole cells was measured with or without dithioerythritol (DTE) in an anaerobic chamber. Cultures were then exposed to air bubbling (0.3 L/h) at room temperature, under shaking conditions. Aliquots (0.5 mL) were withdrawn, and the PFOR catalytic activity was measured anaerobically. After 6 min, aliquots (1 mL) of cultures were withdrawn and extensively bubbled with argon at 35 °C for a further 5 and 10 min before measuring the PFOR activity. For *Dv*H and *Dd*G20 cells, cultures were grown anaerobically in medium C until they reached 0.6−0.8 A_{600} units when they were exposed to air as described previously. *Ca* was grown anaerobically until A_{600} was equal to 1 and then bubbled with air for 6 min until the redox potential was stabilized.

For exposure to H_2O_2, *Da* cells were grown as described previously, and 1 mM H_2O_2 (final concentration) was added to 80 mL of culture under shaking conditions at room temperature. Aliquots (0.5 mL) were periodically collected to measure the PFOR catalytic activity. Changes in the redox potential of the medium were measured using a combined redox electrode, and the O_2 concentration after air bubbling was measured using an oxygen sensor cellox 325 (WTW).

Enzyme Assays. For *Da*, *Dv*H, and *Dd*G20, the PFOR activity was determined as described previously (*8*). One unit of enzyme activity was defined as the amount of enzyme that catalyzed the oxidation of 1 μmol of pyruvate or the reduction of 2 μmol of methyl viologen per minute. To measure the PFOR activity in whole cells, the cell suspension was directly injected into the serum-stoppered cuvettes, and EDTA was added to a final concentration of 4 mM for *Da* and 16 mM for both *Dv*H and *Dd*G20. Catalytic activities of recombinant PFOR and variants were directly measured in soluble extracts of *E. coli*. The *Ca* PFOR activity was measured in crude extracts under anaerobic conditions at 40 °C in 1 mL serum-stoppered cuvettes containing 5 mM sodium pyruvate, 0.1 mM sodium CoA, 2 mM methyl viologen MV, 16 mM DTE, and 100 mM Tris-HCl (pH 7.6). Only a weak endogenous MV reductase activity, neither pyruvate- nor CoA-dependent, was detected in the *Ca* cells. *Ca* crude extracts were prepared from anaerobic cultures (1 L) as described before for the preparation of *E. coli* extracts except that the pellet was resuspended in 1 mL of 100 mM Tris-HCl (pH 7.6).

Analytical Procedures. SDS-PAGE was performed as reported previously (*21*). For in-gel PFOR quantification, 0.04 UOD_{600} cells were loaded onto 7% (w/v) SDS-PAGE gel and electrophoresed. Gels were stained with the Page Blue protein staining solution (Fermentas, conventional

```
     1079                                                                                                  1154
       ↓                                                                                                     ↓
Da     GMGKSQDVMN TAVKSGYWPL FRYDPRLAAQ GKNPFQLDSK APDGSVEEFL MAQNRFAVLD RSFPEDAK-- --RLRAQVAH
Dg     GMGKTQEEGK QATLSGYWPL FRYNPMLLAE GKNPFQLDSK APDGTVQDFL GGESRFSMLE RSHPVAAKPP TSRLRCEIEA
DvH    GMGKSMEEGK LAVESGYWPL YRFNPELADQ GKNPFVLESK APDGTMQDFL AGENRYALLE KIAPEESK-- --RLRAQIEK
DdG20  GMGKSMEEGK LAVETGYWPL YRFNPELADE GKNPFIFESK APNGEIQEFL SGENRYALLE KMAPEESK-- --RLRMQIEE
Df     GMGKSMEEAK LAVETGYWPL YRFNPELAAE GKNPLTIDSK APAGDFQGFL GGEVRYAALE KMHPDMSL-- --RYRTTMEA
Ca     GMGTSIAQEK KAVEAGYWHL YRYNPLLKEQ GKNPFILDSK EPTESYTDFI NGELRYSSLK TIFPDKVE-- --DAFNKSAE
       ***.:    :  *. :*** * :*::* *  : ****: ::**  *      *:  .: *:: *.    *

     1155                                                1195     1203       1212                  1232
       ↓                                                   ↓        ↓          ↓                     ↓
Da     ELDVRFKELE HMAATNIFES FAPAGGKADG SVDFGEGAEF CTRDDTPMMA RPDSG-EACD QNRAGTSEQQ GDLSKRTKK
Dg     QVKARYARLK AMAEAPVLEE ACEL---AKV SMPAAPAPEF CTLTETAEHA RPEEG-APCD AS-------- ---------
DvH    EYVERYSMLK QMAEAPAVTA APGAP----- VAAAGEAGEN CTVSETPEHA RTNGG-SACD DGRSGK---- ---------
DdG20  EYKERYEYMK ALAEMPGFKA EASAP----- VPAGPDAGDA CEVTATPEHA HDAAAGEACN DGRNGK---- ---------
Df     AYKKRYKELE YLASMPVFDA PAAPK----- TGSGDADSAF CEAAPVAEHA RPAAG-EPCD EGRSGK---- ---------
Ca     NAKERYSLYK KLSELQ---- ---------- ---------- ---------- ---------- ---------- ---------
           *:    :  ::     .                          *    ..  * :    .    *  .
```

FIGURE 2: Multiple alignment of the C-terminal sequences of *Desulfovibrio* PFORs. The sequence alignment was obtained using the ClustalW program. Amino acids are numbered based on the *Da* PFOR sequence. The residues shaded in black denote mutated residues in *Da* PFOR of the present study. *Da*: *Desulfovibrio africanus*; *Dg*: *Desulfovibrio gigas*; *Dv*H: *Desulfovibrio vulgaris* Hildenborough; *Dd*G20: *Desulfovibrio desulfuricans* G20; *Df*: *Desulfovibrio fructosovorans*; and *Ca*: *Clostridium acetobutylicum* ATCC824. *Dv*H (*24*), *Dd*G20 (www.tigr.org), and *Ca* (*25*) PFOR sequences were obtained from genome sequences. *Dg* and *Df* PFOR sequences were directly sequenced from genomic DNA.

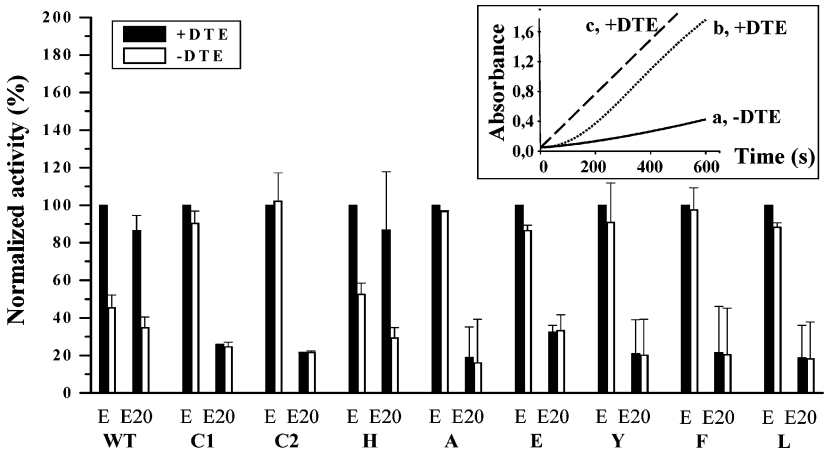

FIGURE 3: Effect of mutation on *Da* PFOR activity. Catalytic activities of PFOR and PFOR variants were measured by injection in a serum-stoppered cuvette of 0.5−2 μL of *E. coli* soluble extracts prepared under oxidative conditions (E) and then aerated for 20 h on ice (E20). Normalized activities were calculated as the fraction of specific activity with or without DTE at each time relative to specific activity with DTE on soluble extracts (100%). For all PFOR variants, the values of the specific activity for the 100% point ranged from 0.8 to 1.2 U/mg. WT corresponds to recombinant *Da* PFOR and C1 and C2 to Cys1195Ala and Cys1212Ala substitutions, respectively. H, A, E, Y, F, and L stand for Met1203His, Met1203Ala, Met1203Glu, Met1203Tyr, Met1203Phe, and Met1203Leu, respectively. Inset: kinetics of the pyruvate-dependent MV reduction by recombinant *Da* PFOR. (a and b) Kinetics of *E. coli* soluble extracts prepared in oxidative conditions and (c) kinetics of *E. coli* soluble extracts prepared in anaerobic conditions.

protocol). Finally, stained gels were scanned using the ImageScanner system from APBiotech, and densitometric analyses were performed using the ImageMaster 2D software (APBiotech). The protein concentration was measured using the method of Lowry et al. (*22*). Total protein concentration was determined from the cell suspension using the modified Lowry protein assay as described previously (*23*).

RESULTS

Specification of the Da PFOR Protective Mechanism. Previous data have suggested the involvement of the C-terminal region of PFOR from *Da* cells providing oxygen stability (*10*). The protein dimer structure shows that the last 62 residues of one subunit form an extra disulfide bond-containing domain that covers the proximal [4Fe-4S] cluster of the other subunit (Figure 1, ref *12*). All *Desulfovibrio* PFOR sequences analyzed contained a C-terminal extension, with two highly conserved Cys residues, C1195 and C1212 (*Da* PFOR numbering) involved in the disulfide bond formation of *Da* PFOR (Figure 2). To investigate the role of these two Cys residues in the oxygen stability of the enzyme, each Cys was replaced by an Ala residue using site-directed mutagenesis. Soluble extracts of *Da* WT PFOR, produced in *E. coli* and prepared under oxidative conditions, displayed the same pyruvate-dependent MV reduction kinetics as the enzyme isolated from *Da* [Figure 3, inset (a and b)]. In particular, the kinetics obtained in the presence of DTE showed an induction period related to an activation process of PFOR as previously postulated (*8*). This led to a lower PFOR activity in the absence of DTE. After 20 h exposure to air, the *E. coli* extracts displayed around 87% of the initial PFOR activity with a similar DTE-dependent activation process (Figure 3). When soluble extracts were prepared anaerobically, no induction was observed [Figure

3, inset (c)], and the kinetics obtained with or without DTE was similar. Moreover, activities remained stable during 20 h (data not shown). Preparation of *E. coli* soluble extracts under oxidative conditions induced a reversible deactivation of the WT PFOR, leading to a less active but stable form of the enzyme toward oxygen. Native PFOR and that produced in *E. coli* therefore exhibited the same activity characteristics, thus validating the site-directed mutagenesis strategy in *E. coli*.

The two PFOR variants (C1195A and C1212A) showed similar expression in *E. coli* to WT PFOR with no significant difference in PFOR activity found in anaerobic extracts (data not shown). With extracts prepared under oxidative conditions, no DTE-dependent activation was measured for either variant (Figure 3). Activities identical to WT PFOR in the presence of DTE indicated an oxidative soluble extract preparation too weak to induce any enzyme damage. However, after 20 h of air exposure, only ~22% of initial activity was recovered in the absence and there was no increase in the presence of DTE, whereas ~87% of the activity was recovered in WT PFOR (Figure 3). These results demonstrate that without disulfide bond formation, the PFOR activity is irreversibly lost in oxidative conditions. The disulfide bond is thus required to maintain an oxygen stable but less active form that can be fully reactivated by DTE.

Once the disulfide bond is formed, the PFOR structure highlights a Met residue (M1203) in close vicinity to the proximal [4Fe-4S] cluster (Figure 1, ref *12*). We substituted this hydrophobic residue with either a neutral (Ala), negatively charged (Glu), or a hydrophobic residue (Tyr, Phe, or Leu). For all replacements, the anaerobic soluble extracts displayed a PFOR activity similar to that of the WT PFOR, stable over 20 h (data not shown). After 20 h exposure to air, only ~20% of the initial PFOR activity was measured with no DTE-dependent activation observed (Figure 3). This irreversible loss of PFOR activity with all three hydrophobic residues indicates that the hydrophobic character of the residue at position 1203 is not sufficient to offer oxygen stability. As Met 1203 is systematically replaced by a His residue in the four other *Desulfovibrio* species (Figure 2), we introduced the same substitution in *Da* PFOR (M1203H). After 20 h exposure to air, soluble extracts containing the M1203H PFOR exhibited 29.5 ± 5% of the initial PFOR activity in the absence of DTE, and 83 ± 20% of the activity was recovered in the presence of DTE (Figure 3).

These experiments show that the formation of the disulfide bond in the C-terminal domain of the PFOR and the presence of a Met or His residue at position 1203 are required for an oxygen stable enzyme. The disulfide bond formation/cleavage is a protective mechanism that switches the enzyme from a fully active oxygen-sensitive form to a less active but oxygen stable form.

Effect of Oxidative Stress on PFOR Activity in Vivo. Is this disulfide bond-dependent protective switch efficient in vivo? To answer this question, we exposed *Da* cells to air bubbling and analyzed the effects on PFOR activity in the whole cells. As a control, we measured endogenous MV reductase activity, which was negligible and neither pyruvate nor CoA dependent. No observed DTE-dependent activation prior to air bubbling of the culture indicated a fully active form of PFOR (Figure 4A). During air bubbling, the PFOR activity gradually decreased with time. However, a full recovery of activity was possible with the addition of DTE. We observed a maximum decrease in activity after 6 min of air bubbling corresponding to the maximum increases in redox potential and O_2 concentration in the medium (Figure 4A,C). It should be noted that PFOR remained fully active in cells kept in anaerobic conditions over this time period (data not shown). These data indicate that air bubbling leads to an oxygen-resistant form of the enzyme in the whole cells, which retains around 20% activity. As H_2O_2 is able to oxidize thiol groups (*26*), we analyzed the effect of hydrogen peroxide on PFOR activity in vivo. With the addition of 1 mM H_2O_2 to the *Da* anaerobic culture, the PFOR activity declined to 26 ± 10% after 6 min exposure. Full activity was restored (102 ± 12%) following the addition of DTE in the serum-stoppered cuvette.

Taken together, these results indicate that oxidative conditions induce the disulfide bond-dependent protective switch of the PFOR in *Da* cells. We then wanted to determine as to whether this mechanism is reversible in vivo. For this, we exposed cultures to air for 6 min, as described previously, and then shifted cultures to more reducing conditions by continuous bubbling with argon at 35 °C. The PFOR activity increased with time during bubbling, reaching a value close to the one measured with DTE (Figure 4A). To check that this increase of PFOR activity did not arise from de novo synthesis of the enzyme, the amount of PFOR was quantified by densitometry after visualization on SDS-PAGE (Figure 4B). Note that we cannot add chloramphenicol in *Da* cells because this antibiotic interferes directly with PFOR activity measurements. No significant variation in the amount of PFOR was observed during the experiment (Figure 4B). These results show unambiguously that the enzyme switched to its fully active form when conditions became less oxidative. In *Da*, this disulfide bond-dependent protective switch of PFOR is thus efficient and reversible in vivo.

Existence of a Protective Mechanism in Other Desulfovibrio PFORs. Desulfovibrio PFORs exhibit an extension at the C-terminus homologous to that of *Da* PFOR (Figure 2). To determine as to whether the protective mechanism occurs in other *Desulfovibrio* species in vivo, we analyzed the PFOR activity in both *Dv*H and *Dd*G20 after air bubbling as described previously. Both *Dv*H and *Dd*G20 PFOR activities decreased, and initial levels of activity were restored with DTE (Figure 5). No DTE-dependent activation was observed when cells were kept in anaerobic conditions. These PFOR activity profiles are thus similar to that described previously for *Da*, indicating that the same disulfide bond-dependent mechanism of protection occurs in these *Desulfovibrio* species. In contrast, *Ca* PFOR activity declined to 0.11 U/mg after 6 min of air bubbling, corresponding to a ~95% activity loss. No recovery to the initial value was obtained after the addition of DTE (0.12 U/mg). As a control, PFOR remained ~100% active (1.9 U/mg) if cells were maintained under nitrogen. This suggests that *Ca* PFOR is irreversibly inactivated by air, a result that reflects the absence of the C-terminal extension including the two cysteine residues (Figure 2), confirming the crucial function of this extra domain in the protective mechanism of PFORs.

DISCUSSION

Previous studies have reported the unusual high stability of *Desulfovibrio africanus* PFOR toward oxygen in vitro,

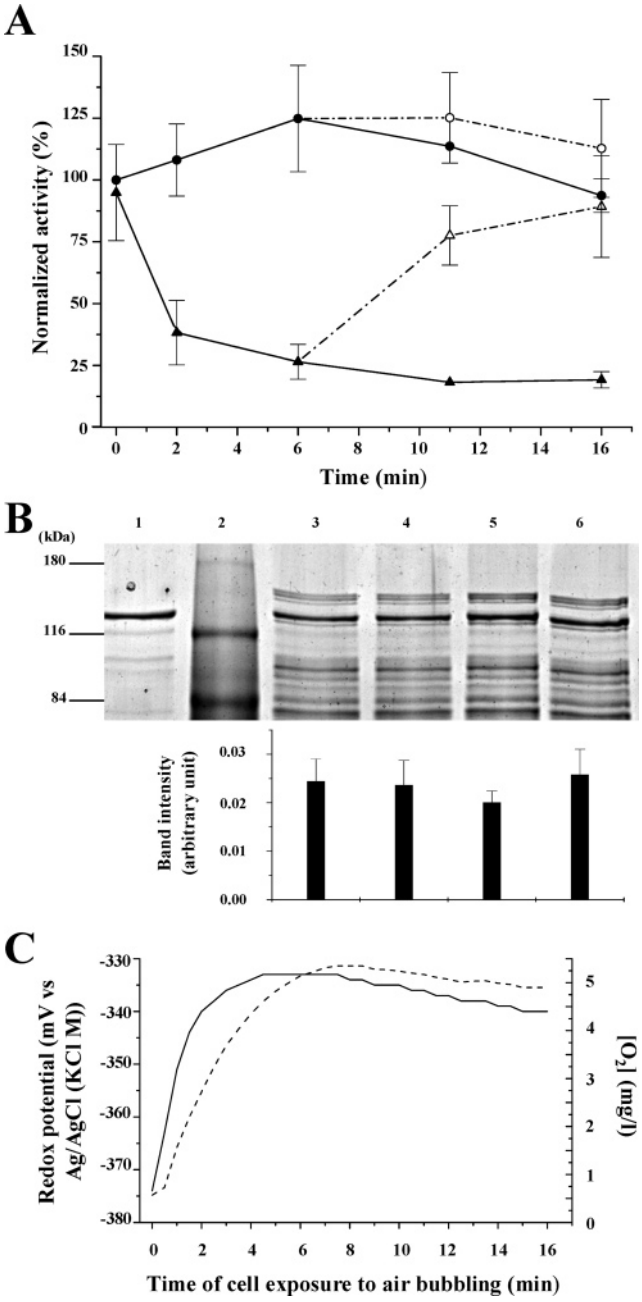

FIGURE 4: Variation of *Da* PFOR catalytic activity during continuous air bubbling of the cells in vivo and recovery of reductive conditions by continuous argon bubbling. (A) Catalytic activities with (●) or without (▲) DTE in aerated cells (solid lines) were measured at various times following the injection of 25 μL of culture in a serum-stoppered cuvette. After 6 min of air bubbling, catalytic activities [with (○) or without (△) DTE] were also measured in cells shifted to reductive conditions at 35 °C by argon bubbling (dashed lines). Normalized activities were calculated as fractions of the specific activity with or without DTE at each time relative to the specific activity with DTE of unstressed cells (100%, ~0.8 U/mg). (B) SDS-PAGE 7% gel. Lane 1: 2 μg of purified PFOR from *Da*; lane 2: molecular weight markers (SDS 7B, Sigma); lane 3: 0.04 UOD_{600} of anaerobic cells; lane 4: 0.04 UOD_{600} of aerated cells for 6 min; and lanes 5 and 6: 0.04 UOD_{600} of cells shifted to reductive conditions by argon bubbling for 5 and 10 min, respectively. Histograms represent the PFOR band intensity, quantified by densitometric analysis for each lane. We previously verified that the protein amount loaded on the gel is proportional to the band intensity after staining. (C) Redox potential [mV vs Ag/AgCl (KCl 3 M), solid line] and O_2 concentration (dashed line) of the medium were measured during continuous air bubbling. Time corresponds to time of cell exposure to air bubbling.

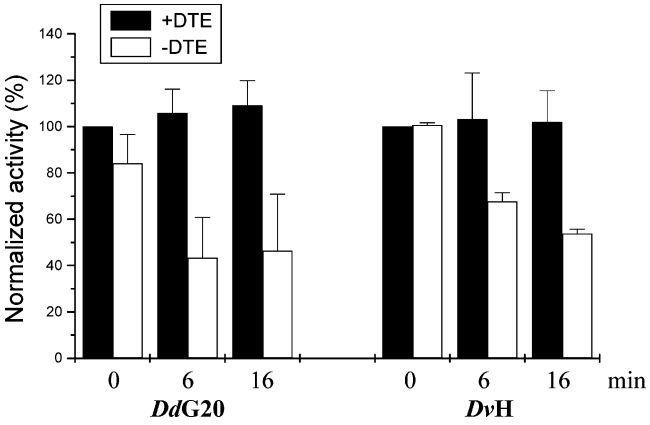

FIGURE 5: Variation of *Dd*G20 and *Dv*H PFOR catalytic activity in vivo during continuous air bubbling. Catalytic activities were measured in aerated cells at various times (0, 6, or 16 min) by injection of 25 μL of culture in a serum-stoppered cuvette. Normalized activities were calculated as the fraction of the specific activity with or without DTE at each time relative to specific activity with DTE of unstressed cells (100%, ~0.08 and ~0.15 U/mg for *Dd*G20 and *Dv*H, respectively).

as compared to homologous PFORs isolated from other anaerobic organisms (*8*, *10*−*13*). On the basis of the *Da* PFOR crystal structure and sequence alignments of *Desulfovibrio* PFOR (Figures 1 and 2), we replaced conserved Cys residues C1195 and C1212 as well as Met1203 by site-directed mutagenesis. The effects of these substitutions on the catalytic activity of the enzyme were analyzed both in anaerobic and in oxidative conditions. When either Cys residue is replaced to impair the formation of the disulfide bond, the protein is more sensitive to oxygen and nonreactive to DTE. Formation of a disulfide bond between both Cys residues is therefore crucial for enzyme protection in oxidative conditions. By analyzing the effect of replacing Met, we have confirmed the hypothesis that the disulfide bond formation is associated with a conformational change allowing the protection of the proximal [4Fe-4S] cluster through this residue (ref *12*, Figure 1). A drastic effect on the stability of the PFOR after air exposure was observed following all replacements except His (Figure 3). The stability of the variant M1203H can be correlated to the presence of a His at this position in all known sequences of *Desulfovibrio* PFOR (Figure 2). Replacement of Met by a small (Ala) or a hydrophilic (Glu) residue should have resulted in a greater degree of solvent accessibility of the proximal [4Fe-4S] cluster, making it in turn more sensitive to oxidative damage. Substituting Met with hydrophobic and bulky residues (Tyr, Phe, and Leu) also led to oxygen sensitivity. This result is more surprising because previous studies report that in iron-sulfur proteins, bulky residues in the vicinity of the [4Fe-4S] cluster are generally involved in protecting the cluster from the solvent (*13*, *27*, *28*). Overall, our data show that the protective mechanism of *Da* PFOR depends crucially on the presence of M1203. It has previously been proposed that Met residues act as endogenous antioxidants (*29*). In *Da* PFOR, M1203 could act as an efficient oxidant scavenger, structurally arranged to guard the proximal cluster against the entrance of oxidants. We propose that PFOR is able to switch, through a disulfide bond formation-dependent process, from a high activity oxygen-sensitive form to a low activity oxygen-protected form. The

Da enzyme would take advantage of the [4Fe-4S] cluster protection but, in return, must lower its catalytic activity.

Moreover, we have demonstrated that this disulfide bond-dependent protective switch is efficient and reversible in vivo after an oxidative stress induced by either air or H_2O_2. To our knowledge, this is the first example of the formation of an intramolecular disulfide bridge as a protective switch for an enzyme. An important question is how the disulfide bond in *Desulfovibrio* PFORs could be formed in the cells. Efforts to address this question are underway. Accumulation of reactive oxygen species can cause specific protein modifications that may lead to a change in the activity or function of the oxidized protein. For example, H_2O_2 directly oxidizes protein thiols to adjust the activity of various transcription factors or molecular chaperones (*30*−*33*). However, spontaneous or enzyme-assisted generation of disulfide bonds, during oxidative stress, in the normal resident proteins of the cytosol such as PFOR has to be demonstrated. We also cannot exclude the involvement of the proximal [4Fe-4S] cluster in the formation of the disulfide bond by a redox exchange between iron and local cysteine residue as suggested by the close distance between them (*12*). Such an electron transfer has been recently reported in other redox proteins (*34*, *35*).

The protective mechanism appears not to be restricted to the *Da* PFOR as it is also efficient in vivo in *Dv*H and *Dd*G20 cells. In contrast, *Ca* irreversibly loses ∼95% of its PFOR activity during aeration in accordance with lacking the two conserved Cys residues in its sequence. In the same way, a total irreversible loss of PFOR activity in vivo is observed in the obligate anaerobe *Bacteroides thetaiotaomicron* following a long period of exposure to air (*36*). From our site-directed mutagenesis study and analysis of in vivo catalytic activity, we propose that the protective mechanism described here for *Da* PFOR exists for all *Desulfovibrio* PFORs through the use of either a Met or a His residue as the primary shield against cluster disintegration by oxidative damage.

The presence of communities of sulfate-reducing bacteria (SRB) in oxic environments has been widely reported, particularly in the oxic/anoxic interface of microbial mats or sediments as well as in periodically oxygenated zones of aquatic environments (reviewed in ref 37). This new mechanism of protection of one of the key enzymes implicated in the central metabolism of these strict anaerobes could be considered as an adaptation strategy used by SRB to cope with temporary exposure to oxidative conditions. In 1979, Postgate wrote that when exposed to air, SRB "....will not be killed, but will remain dormant" (*38*). Later, LeGall and Xavier (*39*) proposed that *Desulfovibrio* species seem to be capable of "active dormancy" (as opposed to sporulation as "passive dormancy"). The maintenance of cell activity (*39*−*41*) enables such cells to rapidly resume growth on re-entering an anaerobic habitat. The protective mechanism we describe here might be a part of this active dormancy. Oxidation of pyruvate to acetyl-CoA by the oxygen stable form of PFOR could help *Desulfovibrio* perform this "active dormancy". A previous study has shown that pyruvate could be oxidized to acetate in non-growing *D. gigas* cell suspensions under oxygen (*41*). Once the environment returns to more reductive conditions, a high rate of pyruvate oxidation is restored in the cells due to PFOR switching to its fully active form with no de novo PFOR synthesis, thus allowing quick growth recovery.

REFERENCES

1. Evans, M. C., Buchanan, B. B., and Arnon, D. I. (1966) A new ferredoxin-dependent carbon reduction cycle in a photosynthetic bacterium, *Proc. Natl. Acad. Sci. U.S.A. 55* (4), 928−934.
2. Tersteegen, A., Linder, D., Thauer, R. K., and Hedderich, R. (1997) Structures and functions of four anabolic 2-oxoacid oxidoreductases in *Methanobacterium thermoautotrophicum*, *Eur. J. Biochem. 244* (3), 862−868.
3. Ikeda, T., Ochiai, T., Morita, S., Nishiyama, A., Yamada, E., Arai, H., Ishii, M., and Igarashi, Y. (2006) Anabolic five subunit-type pyruvate/ferredoxin oxidoreductase from *Hydrogenobacter thermophilus TK-6*, *Biochem. Biophys. Res. Commun. 340* (1), 76−82.
4. Lin, W. C., Yang, Y. L., and Whitman, W. B. (2003) The anabolic pyruvate oxidoreductase from *Methanococcus maripaludis*, *Arch. Microbiol. 179* (6), 444−456.
5. Furdui, C., and Ragsdale, S. W. (2000) The role of pyruvate ferredoxin oxidoreductase in pyruvate synthesis during autotrophic growth by the Wood−Ljungdahl pathway, *J. Biol. Chem. 275* (37), 28494−28499.
6. Kletzin, A., and Adams, M. W. (1996) Molecular and phylogenetic characterization of pyruvate and 2-ketoisovalerate ferredoxin oxidoreductases from *Pyrococcus furiosus* and pyruvate ferredoxin oxidoreductase from *Thermotoga maritima*, *J. Bacteriol. 178* (1), 248−257.
7. Zhang, Q., Iwasaki, T., Wakagi, T., and Oshima, T. (1996) 2-Oxoacid: Ferredoxin oxidoreductase from the thermoacidophilic archaeon, *Sulfolobus* sp. strain 7, *J. Biochem. (Tokyo, Jpn.) 120* (3), 587−599.
8. Pieulle, L., Guigliarelli, B., Asso, M., Dole, F., Bernadac, A., and Hatchikian, E. C. (1995) Isolation and characterization of the pyruvate-ferredoxin oxidoreductase from the sulfate-reducing bacterium *Desulfovibrio africanus*, *Biochim. Biophys. Acta 1250* (1), 49−59.
9. Odom, J. R. (1984) *The Sulphate-Reducing Bacteria*, Cambridge University Press, Cambridge, U.K.
10. Pieulle, L., Magro, V., and Hatchikian, E. C. (1997) Isolation and analysis of the gene encoding the pyruvate-ferredoxin oxidoreductase of *Desulfovibrio africanus*, production of the recombinant enzyme in *Escherichia coli*, and effect of carboxy-terminal deletions on its stability, *J. Bacteriol. 179* (18), 5684−5692.
11. Pieulle, L., Chabriere, E., Hatchikian, C., Fontecilla-Camps, J. C., and Charon, M. H. (1999) Crystallization and preliminary crystallographic analysis of the pyruvate-ferredoxin oxidoreductase from *Desulfovibrio africanus*, *Acta Crystallogr., Sect. D: Biol. Crystallogr. 55* (*1*), 329−331.
12. Chabriere, E., Charon, M. H., Volbeda, A., Pieulle, L., Hatchikian, E. C., and Fontecilla-Camps, J. C. (1999) Crystal structures of the key anaerobic enzyme pyruvate/ferredoxin oxidoreductase, free and in complex with pyruvate, *Nat. Struct. Biol. 6* (2), 182−190.
13. Pieulle, L., Nouailler, M., Morelli, X., Cavazza, C., Gallice, P., Blanchet, S., Bianco, P., Guerlesquin, F., and Hatchikian, E. C. (2004) Multiple orientations in a physiological complex: The pyruvate-ferredoxin oxidoreductase-ferredoxin system, *Biochemistry 43* (49), 15480−15493.
14. Chabriere, E., Vernède, X., Guigliarelli, B., Charon, M. H., Hatchikian, E. C., and Fontecilla-Camps, J. C. (2001) Crystal structure of the free radical intermediate of pyruvate/ferredoxin oxidoreductase, *Science (Washington, DC, U.S.) 294* (5551), 2559−2563.
15. Legall, J., Mazza, G., and Dragoni, N. (1965) Cytochrome c_3 of *Desulfovibrio gigas*, *Biochim. Biophys. Acta 99*, 385−387.
16. Postgate, J. R. (1984) *The Sulphate-Reducing Bacteria*, 2nd ed., pp 12−13, Cambridge University Press, Cambridge, U.K.
17. Weimer, P. J., Van Kavelaar, M. J., Michel, C. B., and Ng, T. K. (1988) Effect of phosphate on the corrosion of carbon steel and on the composition of corrosion products in two-stage continuous cultures of *Desulfovibrio desulfuricans*, *Appl. Environ. Microbiol. 54* (2), 386−396.
18. Ochman, H., Medhora, M. M., Garza, D., and Hartl, D. L. (1990) in *Amplification of Flanking Sequences by Inverse PCR*, *PCR Protocols* (Innis, M. A., Gelfand, D. H., Sninsky, J. J., White, T. J., Eds.) pp 219−227, Academic Press, Inc., San Diego.

19. Ho, S. N., Hunt, H. D., Horton, R. M., Pullen, J. K., and Pease, L. R. (1989) Site-directed mutagenesis by overlap extension using the polymerase chain reaction, *Gene 77* (1), 51−59.
20. Nakamura, M., Saeki, K., and Takahashi, Y. (1999) Hyperproduction of recombinant ferredoxins in *Escherichia coli* by coexpression of the ORF1-ORF2-iscS-iscU-iscA-hscB-hscA-fdx-ORF3 gene cluster, *J. Biochem. (Tokyo, Jpn.) 126* (1), 10−18.
21. Laemmli, U. K. (1970) Cleavage of structural proteins during the assembly of the head of bacteriophage T4, *Nature (London, U.K.) 227* (5259), 680−685.
22. Lowry, O. H., Rosebrough, N. J., Farr, A. L., and Randall, R. J. (1951) Protein measurement with the Folin phenol reagent, *J. Biol. Chem. 193* (1), 265−275.
23. Bensadoun, A., and Weinstein, D. (1976) Assay of proteins in the presence of interfering materials, *Anal. Biochem. 70* (1), 241−250.
24. Heidelberg, J. F., Seshadri, R., Haveman, S. A., Hemme, C. L., Paulsen, I. T., Kolonay, J. F., Eisen, J. A., Ward, N., Methe, B., Brinkac, L. M., Daugherty, S. C., Deboy, R. T., Dodson, R. J., Durkin, A. S., Madupu, R., Nelson, W. C., Sullivan, S. A., Fouts, D., Haft, D. H., Selengut, J., Peterson, J. D., Davidsen, T. M., Zafar, N., Zhou, L., Radune, D., Dimitrov, G., Hance, M., Tran, K., Khouri, H., Gill, J., Utterback, T. R., Feldblyum, T. V., Wall, J. D., Voordouw, G., and Fraser, C. M. (2004) The genome sequence of the anaerobic, sulfate-reducing bacterium *Desulfovibrio vulgaris Hildenborough*, *Nat. Biotechnol. 22* (5), 554−559.
25. Nolling, J., Breton, G., Omelchenko, M. V., Makarova, K. S., Zeng, Q., Gibson, R., Lee, H. M., Dubois, J., Qiu, D., Hitti, J., Wolf, Y. I., Tatusov, R. L., Sabathe, F., Doucette-Stamm, L., Soucaille, P., Daly, M. J., Bennett, G. N., Koonin, E. V., and Smith, D. R. (2001) Genome sequence and comparative analysis of the solvent-producing bacterium *Clostridium acetobutylicum*, *J. Bacteriol. 183* (16), 4823−4838.
26. Thomas, J. A., and Mallis, R. J. (2001) Aging and oxidation of reactive protein sulfhydryls, *Exp. Gerontol. 36* (9), 1519−1526.
27. Fukuyama, K., Matsubara, H., Tsukihara, T., and Katsube, Y. (1989) Structure of [4Fe-4S] ferredoxin from *Bacillus thermoproteolyticus* refined at 2.3 Å resolution, *J. Mol. Biol. 210* (2), 383−398.
28. Singh, B. B., Curdt, I., Shomburg, D., Bisen, P. S., and Bohme, H. (2001) Valine 77 of heterocystous ferredoxin FdxH2 in *Anabaena variabilis* strain ATCC 29413 is critical for its oxygen sensitivity, *Mol. Cell. Biochem. 217* (1−2), 137−142.
29. Levine, R. L., Mosoni, L., Berlett, B. S., and Stadtman, E. R. (1996) Methionine residues as endogenous antioxidants in proteins, *Proc. Natl. Acad. Sci. U.S.A. 93* (26), 15036−15040.
30. Zheng, M., Åslund, F., and Storz, G. (1998) Activation of the OxyR transcription factor by reversible disulfide bond formation, *Science (Washington, DC, U.S.) 13*, 1718−1722.
31. Åslund, F., Zheng, M., Beckwith, J., and Stor, G. (1999) Regulation of the OxyR transcription factor by hydrogen peroxide and the cellular thiol disulfide status, *Proc. Natl. Acad. Sci. U.S.A. 96*, 6161−6165.
32. Jakob, U., Muse, W., Eser, M., and Bardwell, J. C. A. (1999) Chaperone activity with a redox switch, *Cell 96*, 341−352.
33. Pop, S. M., Gupta, N., Ashraf, S., Raza, A. S., and Ragsdale, S. W. (2006) Transcriptional activation of dehalorespiration: Identification of redox-active cysteines regulating dimerization and DNA binding, *J. Biol. Chem. 281*, 26382−26390.
34. Walters, E. M., Garcia-Serres, R., Jameson, G. N., Glauser, D. A., Bourquin, F., Manieri, W., Schürmann, P., Johnson, M. K., and Huynh, B. H. (2005) Spectroscopic characterization of site-specific [Fe(4)S(4)] cluster chemistry in ferredoxin. Thioredoxin reductase: implications for the catalytic mechanism, *J. Am. Chem. Soc. 127* (26), 9612−9624.
35. Dai, S., Fiemann, R., Glauser, D., A., Bourquin, F., Manieri, W., Schürmann, P., and Ecklund, H. (2007) Structural snapshots along reaction pathway of ferredoxin-thioredoxin reductase, *Nature (London, U.K.) 448* (7149), 92−96.
36. Pan, N., and Imlay, J. A. (2001) How does oxygen inhibit central metabolism in the obligate anaerobe *Bacteroides thetaiotaomicron?*, *Mol. Microbiol. 39* (6), 1562−1571.
37. Dolla, A., Fournier, M., and Dermoun, Z. (2006) Oxygen defense in sulfate-reducing bacteria, *J. Biotechnol. 126* (1), 87−100.
38. Postgate, J. R. (1984) *The Sulphate-Reducing Bacteria*, 2nd ed., p 208, Cambridge University Press, Cambridge, U.K.
39. Le Gall, J., and Xavier, A. V. (1996) Anaerobes response to oxygen: The sulfate-reducing bacteria, *Anaerobe 2* (1), 1−9.
40. Van Niel, E. W. J., Pedro Gomes, T. M., Willems, A., Collins, M. D., Prins, R. A., and Gottschal, J. C. (1996) The role of polyglucose in oxygen-dependent respiration by a new strain of *Desulfovibrio salexigens*, *FEMS Microbiol. Ecol. 21*, 243−253.
41. Fareleira, P., Santos, B. S., Antonio, C., Moradas-Ferreira, P., LeGall, J., Xavier, A. V., and Santos, H. (2003) Response of a strict anaerobe to oxygen: Survival strategies in *Desulfovibrio gigas*, *Microbiol. 149* (6), 1513−1522.
42. DeLano, W. L. (2002) *PyMOL*, DeLano Scientific, San Carlo, CA.

BI7014713